

# THE TDA8140/43: A SELF-ADAPTING DRIVER CIRCUIT FOR HORIZONTAL TV DEFLECTION

In conventional TV horizontal deflection stages the output transistor is driven by a medium power transistor and a transformer. The disadvantage of this solution is that the drive circuit must be optimized for each application to ensure saturation of the power transistor. Moreover dissipation is higher than necessary because this type of circuit cannot supply the ideal base current. And when the chassis is turned-on or off the power transistor is stressed, compromising reliability.

The SGS TDA 8140 is a new alternative (patent pending) which solves these problems. A small power IC, it provides the optimal charge and discharge currents, adapting to different application conditions. Design is simplified and, because the base current is optimized, dissipation is reduced to a minimum.

Additionally the TDA 8140 includes control and protection functions which enhance system reliability.

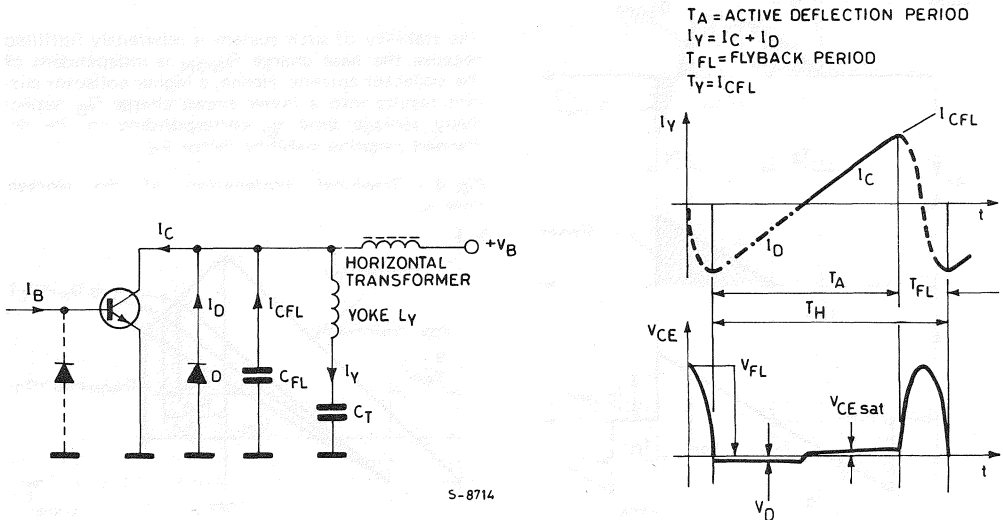
When the chassis is turned ON or OFF, for example, the TDA 8140 ensures that the power transistor is driven correctly. And the TDA 8140 protects both itself and the external power transistor against overload conditions.

The device is available in two packages: a 16-lead DIP package (type TDA 8140) and a 9-lead SIP plastic package (type TDA 8143).

## PRINCIPLE OF OPERATION

A typical deflection circuit of a present chassis is shown in Fig. 1. This concept is realized by an LC resonance circuit which operates at two different frequencies, controlled by the power switch T. One complete deflection period  $T_H$  consists of the active deflection phase  $T_A$  and the flyback phase  $T_{FL}$ . During  $T_A$ , transistor T conducts for positive  $I_Y$ , diode D carries the negative  $I_Y$ .

Fig. 1 - Typical horizontal deflection circuit and related waveforms



Assuming a long period duration of the resonance circuit  $L_T$  and  $C_T$ , compared with  $T_A$ , the deflection current rises quasi linearly. In the flyback phase  $T_{FL}$ , the elements T and D are inactive and the current  $I_Y$  has a cosinus waveshape of a much higher frequency due to the series connection of  $C_T$  and  $C_{FL}$ . The corresponding voltages are determined by a small drop  $V_{CEsat}$  and  $V_D$  during  $T_A$  respectively, the high flyback voltage during  $T_{FL}$ .

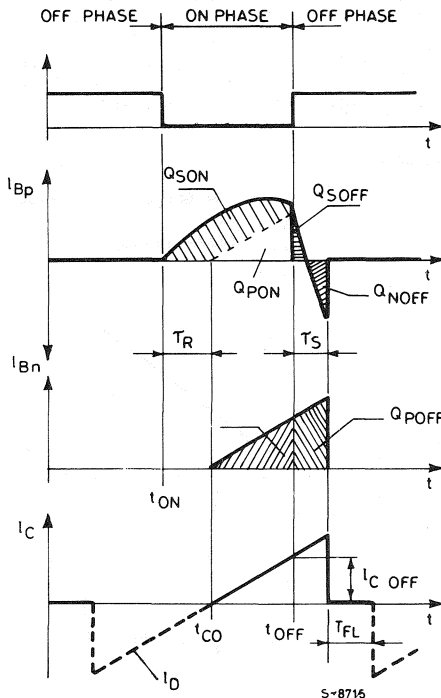
The driver circuit for the power switch must fulfill the different requirements during the ON and OFF phase.

Fig. 2 gives the typical base driving conditions for the power transistor. Normally, the transistor is activated at  $t = t_{ON}$  before the zero crossover of  $I_C$  at  $t_{CO}$ . During the active phase  $t > t_{CO}$ , the transistor must be carefully saturated. This results in an excess base charge  $Q_{SON}$  and leads to the turn OFF delay time  $\tau_S$ .

A typical deflection transistor requires  $V_{CES} > 1500V$  and shows a very low current gain of  $B < 5$  at about  $I_C = 3.5A$ .

An optimum driver circuit represents the trade off between a slow discharge which increases the power dissipation and a fast discharge which is limited by the emitter crowding effect and the reverse second breakdown [1], [2]. The resulting storage time is achieved by a defined base current decay.

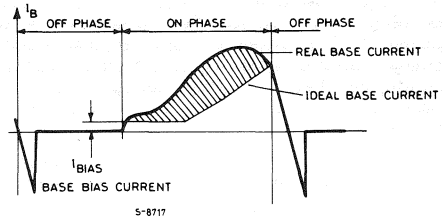
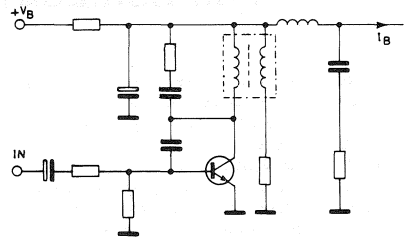
Fig. 2 - Base driving conditions



## DRIVER CIRCUIT CONSIDERATIONS

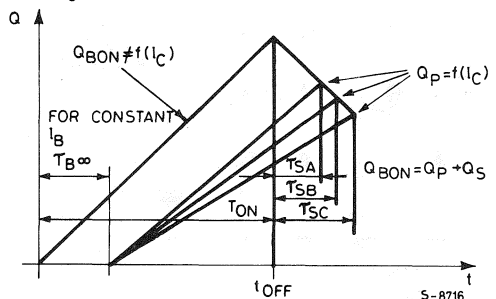
The classical driver circuit in Fig. 3 consists of a discrete transistor and a transformer. During the turn ON phase of the power transistor, the driver is switched off. The current waveform is determined by the primary RC network and is limited by a secondary series resistor. In the turn OFF phase, the negative current slope results from the transformer stray inductance or an additional discrete series coil.

Fig. 3 - Classical driver circuit and output waveform



The stability of such system is inherently fulfilled because the base charge  $Q_{BON}$  is independent of the collector current. Hence, a higher collector current results into a lower excess charge  $Q_S$  respectively storage time  $\tau_S$ , corresponding to the demanded negative stability factor  $K_S$ .

Fig. 4 - Graphical explanation of the storage time  $\tau_S$

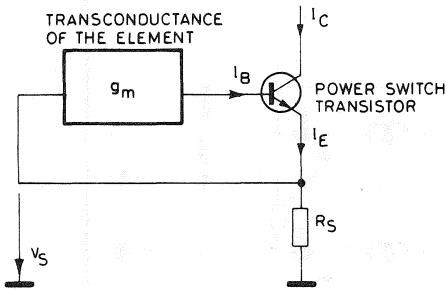


This relationship is illustrated in Fig. 4 for simplified base charges.  $Q_{BON}$  is the actual base charge and  $Q_p$  is the required base charge ensuring saturation for each of the three indicated different collector currents.

## INTEGRATED DRIVER

As explained in the previous chapter, the power transistor in the deflection circuit only operates as a simple switch. Therefore, an optimum driver circuit generates the correct base current in order to guarantee saturation at each instant of time. The dynamic circuit senses the actual current in the power transistor across the emitter resistor  $R_S$ , as shown in Fig. 5 and delivers the base current.

Fig. 5 - Principle of operation of the integrated driver



S-8718

$$I_B = R_S \frac{g_m}{1 - R_S g_m} I_C \quad (1)$$

The saturation condition sets the lower bound for the transconductance  $g_m$ :

$$1/R_S (1 + B_{MIN}) < g_m < 1/R_S \quad (2)$$

whereas the upper bound is given by the stability of the positive feedback loop.

A typical distribution of the current gain versus the collector current for the BU 208A transistor is shown in Fig. 6. The required base current for a minimum beta device defines the transfer characteristics of the driver, approximated by the sum of a constant and a proportional term.

The simplified circuit diagram of such integrated driver circuit (TDA 8140/43) is shown in Fig. 7. It illustrates both, the signal transfer behaviour and auxiliary protection functions.

In the normal operating mode, the control input determines two different conditions:

For a Low input,  $Q_5$  is On and the element acts as a static transconductance amplifier which ensures the proper saturation of the external power

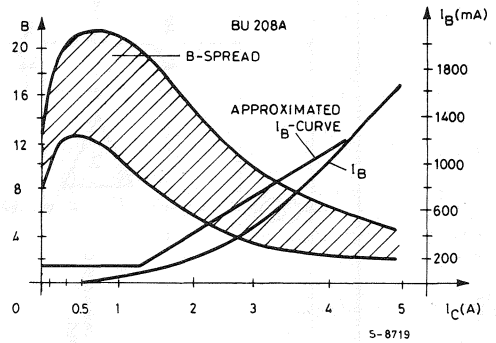
transistor. A High input control signal opens  $Q_5$  and results into an output current ramp, discharging the base of the external transistor.

$$\frac{dI_B}{dt} \sim - \frac{1}{C_{EXT}} \quad (3)$$

Different safety functions enable the output power amplifier:

- 1) During the flyback phase, where the SYN DET input is High
- 2) For supply voltages less than 7V
- 3) For chip temperature higher than 160°C

Fig. 6 - Current gain and base current of the BU208



S-8719

## TRANSCONDUCTANCE AMPLIFIER

The main part of the element consists of a push-pull power transconductance amplifier which can deliver an output current of  $\pm 1.5A$  for a wide output voltage range. This amplifier is a 3 stage design. A ground compatible input stage  $Q_1 \div Q_4$  realizes a transconductance preamplifier with symmetrical output:

$$g_{m1} = \frac{I_1 - I_2}{V_S - V_{CEXT}} = \frac{1}{R_3} \quad (4)$$

The output current  $I_1, I_2$  is fed into the load resistors  $R_1 = R_2$ . Due to the feedback configuration of the further amplifiers  $A_1$  and  $A_2$ , the main output current drop  $I_B \cdot R_5$  becomes equal to the difference voltage across  $R_1$  and  $R_2$ .

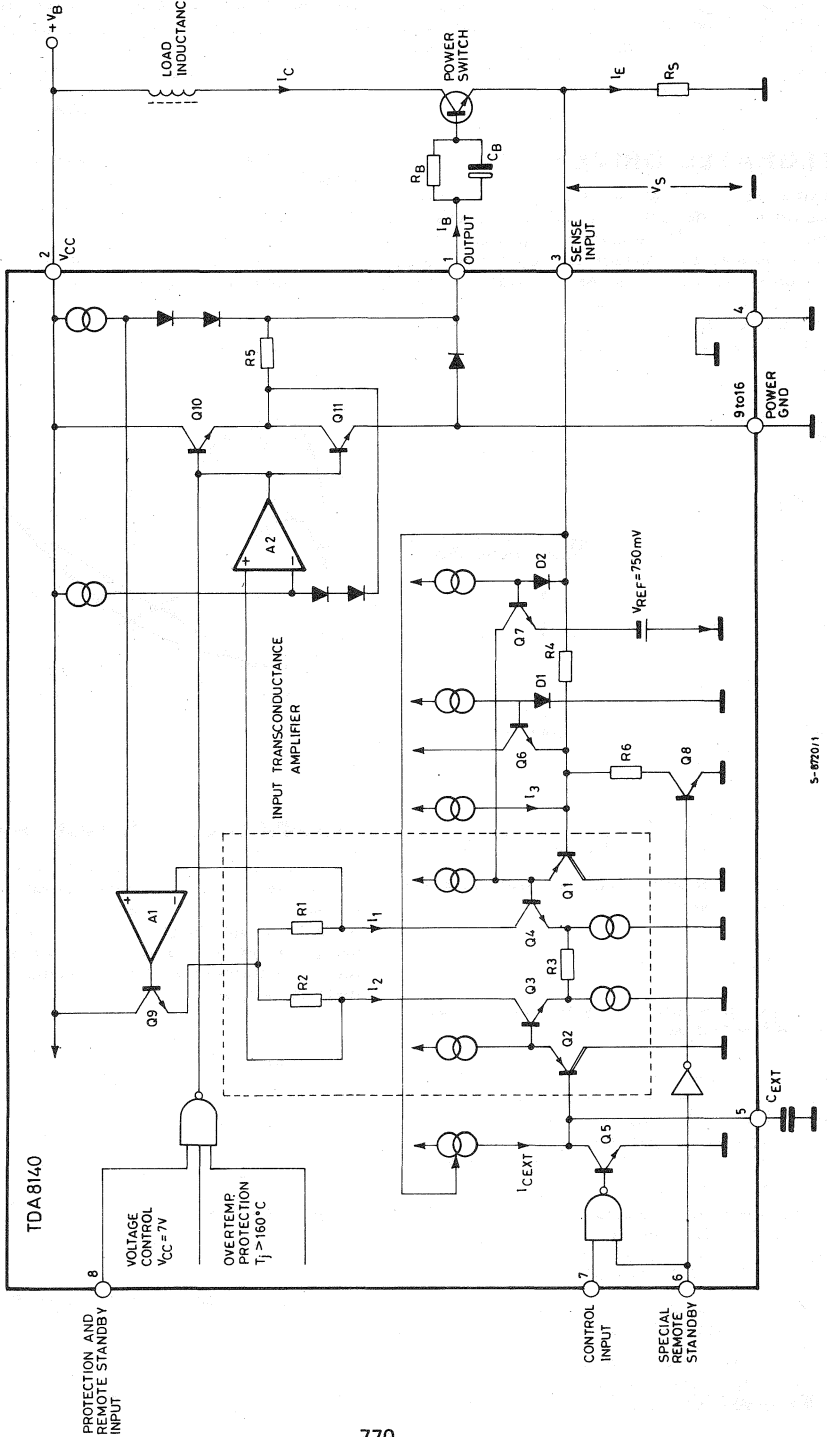
Thus, the overall transfer function  $g_m$  results into:

$$g_m = I_B/V_{IN} = 2 \cdot g_{m1} R_1/R_5 \quad (5)$$

this gives:

$$g_m = 2 \cdot R_1/R_3 R_5 \quad (6)$$

Fig. 7 - Simplified circuit diagram



5-87201

The output current can be expressed as:

$$I_B = (V_S - V_{CEXT}) \cdot 2 \cdot R1/R3 R5. \quad (7)$$

Although the amplifiers A1 and A2 perform a positive feedback configuration, the stability of this inner loop is always ensured. As to be seen from Fig. 8, which gives a simplified structure, the additional amplifier A1 forces an inner voltage at node A, which must be identical to the output voltage at node B. Because the output power amplifier A2 has unity gain, the drop across R5 is equal to the drop across R1 + R2 which results into Eq. (7).

Considering the high output impedance of the first stage, the amplifier A1 also provides unity closed

loop gain, thus the inner loop gain  $v_L$  becomes:

$$v_L = v_{A1} \cdot v_{A2} \cdot \frac{R_L + R_S}{R5 + R_L + R_S} \quad (8)$$

Careful attention is paid to the frequency compensation of A1 and A2 in order to ensure:

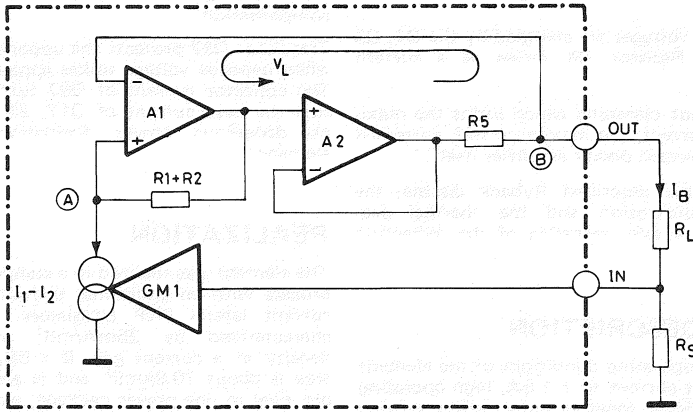
$$v_{A1} = v_{A2} \leq 1. \quad (9)$$

Hence, the loop gain  $v_L$  always becomes:

$$v_L < 1, \quad (10)$$

which guarantees the stability of the inner auxiliary loop  $v_L$ .

Fig. 8 - Simplified signal transfer block diagram



S - 8721

## SYSTEM STABILITY

A controlled base current, proportional to the collector current, does not offer stability because the excess charge is reduced with a decreased collector current. Hereby, the new element would cause instability. However, such characteristic is avoided by a controller base discharge procedure. The slope of the output base current is controlled by the emitter current of the power transistor itself. As to be seen in Fig. 7, the input voltage  $V_S$  determines the charging current  $I_{CEXT}$  of  $C_{EXT}$  via a controlled current source  $g_2$ . Using:

$$I_{CEXT} = g_2 \cdot V_S, \quad (11)$$

the slope  $dI_B/dt$  derived from (7), becomes:

$$\frac{dI_B}{dt} = - \frac{2 \cdot R1}{R3 R5} \frac{dV_{CEXT}}{dt} \quad (12)$$

which results into:

$$\frac{dI_B}{dt} = - \frac{2 \cdot R1}{R3 R5} \frac{g_2 \cdot V_S}{C_{EXT}} \quad (13)$$

A high collector current of the power transistor therefore generates a fast discharge combined with a small storage time and vice versa; consequently, the system stability is obtained.

During the turn OFF phase,  $V_S$  is quasi constant because the collector current is still increasing, whereby the base current is reduced as described.

## AUXILIARY FUNCTIONS

In order to start the regenerative loop together with the power transistor, the element delivers a constant current of 150mA at the output. This proportion is independent of the input voltage and is derived from the constant current source I<sub>3</sub>. The current I<sub>3</sub> provides a 70mV drop across R4 as a prebias of Q1.

In the standby mode, resistor R6 is activated by the saturated transistor Q8. Both, the transconductance and the output DC current are now reduced by a factor of 3.

The operating range of the element is fixed by an input limiting circuit. For input voltages higher than 750mV, D2 activates Q7 which limits the base voltage of Q4. Therefore, the maximum output current is limited to:

$$I_{BMAX} = \frac{750mV}{R_S} \quad (14)$$

Negative input voltages are clamped by the D1, Q6 configuration. Resistor R4 serves as a current limitation.

Beside this input clamping which limits the maximum source current, the maximum sink current is limited in the output power amplifier itself.

Furthermore, the described flyback disable, the undervoltage protection and the thermal protection ensure a safe operating of the deflection system.

## CIRCUIT DESCRIPTION

Some extreme operating conditions of the element like high output current of ± 1.5A, high operating frequency > 15kHz together with a short settling time of a few μs, high substrate current as well as low drift result into an unconventional circuit design and require a careful layout.

## OUTPUT POWER AMPLIFIER

The circuit diagram of the output power amplifier is given in Fig. 9. Transistors Q12, Q13, Q25, Q26, Q63 and Q16 realized a single pole amplifier which is followed by a push-pull output buffer. The upper half is built by the emitter follower Q22 and the output darlington Q17, Q21. The maximum output voltage as a current source is given by  $V_{CC} - V_{BE17} - V_{BE21} - V_{CE5}$ ; the minimum results from the saturation of Q64.

The lower half of the output stage consists of Q36, Q48 and Q66 as active element, where Q41, Q43 and Q34 serve as biasing structures.

The minimum output voltage in the current sink mode is only limited by the saturation voltage of Q66 which is less than 1.2V at 1.5A output current. A low drop current limitation at 2.5A is included in the emitter of Q66 which senses the drop across a 60mΩ metal resistor.

The fast settling of this output amplifier requires a quiescent current of about 10mA. With respect to the temperature stability of this current, the current densities of the related elements fulfill the cancellation condition:

$$\frac{I_{17}}{A_{17}} \cdot \frac{I_{21}}{A_{21}} \cdot \frac{I_{48}}{A_{48}} \cdot \frac{I_{36}}{A_{36}} = \quad (15)$$

$$= \frac{I_{41}}{A_{41}} \cdot \frac{I_{43}}{A_{43}} \cdot \frac{I_{22}}{A_{22}} \cdot \frac{I_{34}}{A_{34}}$$

A 350mΩ emitter diffused resistor R37 realizes the output current sense element. Using a double diode level shift - Q37/38 and Q40/42 - the drop voltage can be applied to a standard PNP differential amplifier. Thus slow input PNP elements can be avoided. Additionally, a clamping circuit Q14, Q23 prevents the forward polarization from the diode C4 which is used for the frequency compensation.

Transistor Q87 protects the upper power transistor when negative voltage spikes appear at the output. The collector current of Q87 turns Q5 off which cuts the base current of Q17, 21. By this means, no dangerous power dissipation imperils the element.

## REALIZATION

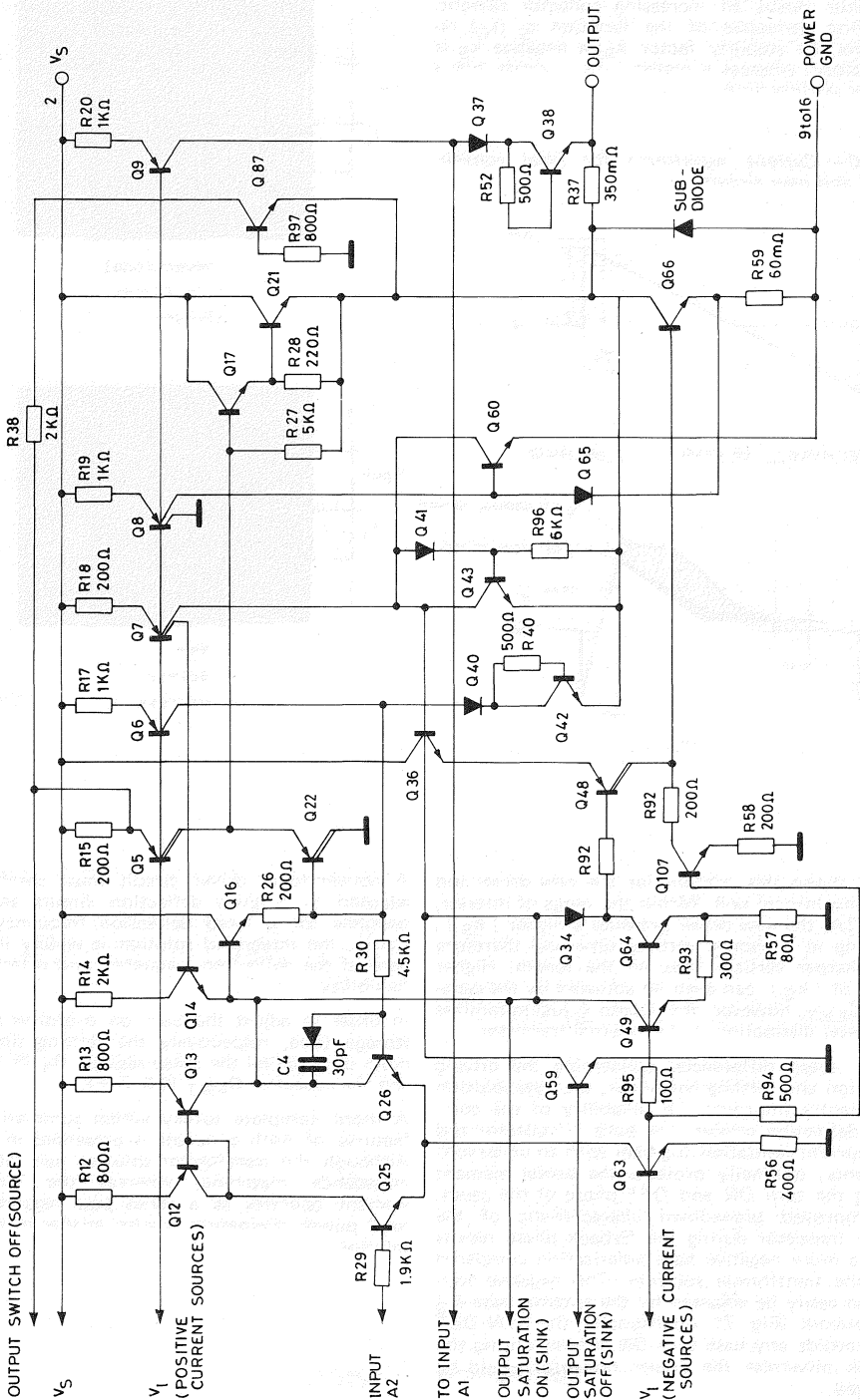
The element was realized in a standard 18V  $V_{BCEQ}$  process with an additional diffusion step for high current lateral PNP transistors. The process is characterized by 25mA/mil<sup>2</sup> emitter current density at a current gain  $B = 5B_{MAX}$ . The chip area is about 10.8kmil<sup>2</sup> and is assembled in a 16 pin dual in line power package, where one side of the leads is used for heat sink. This package has a thermal resistance of 15K/W (chip to leads).

## EXPERIMENTAL RESULTS AND COMPARISON TO THE DISCRETE DRIVER

The performance of the TDA 8140/43 integrated driver has been investigated both theoretically and experimentally. The collector current of the power transistor, together with the related base current for the ideal case, the conventional driver and the new one is presented in Fig. 10. A significant difference is clearly visible in the hatched area, representing the excess base charge. The new driver nearly the classical driver provides only a rough approximation of this objective function due to the limit number of components.

The practical results confirm this described difference. Fig. 11 shows the measured collector and base currents for the conventional driver (top) and for the new driver (bottom), applied in the same chassis.

Fig. 9 - Complete output power stage



S-8759

As discussed above, the stability of the deflection requires a decreasing storage time  $\tau_s$  of the power transistor versus an increasing collector current. The first derivative of the function  $\tau_s(I_C)$  represents the stability factor  $k_S$ ; a negative  $k_S$  is mandatory, whereas a higher  $|k_S|$  yields into a shorter settling time.

Fig. 10 - Current waveforms for ideal conventional and new circuit

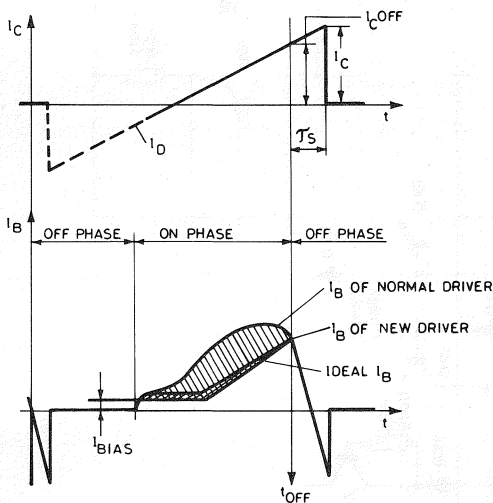
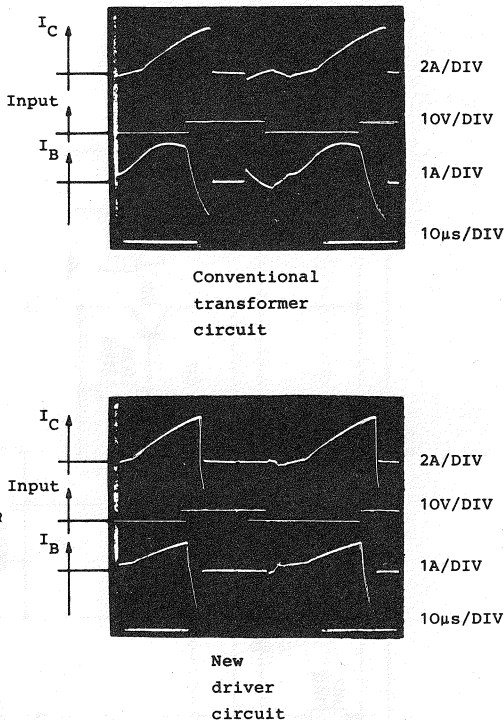


Fig. 2 shows this relation for the new driver and the conventional one. Within the range of interest,  $I_C \approx 3A$ , the new driver provides a higher  $|k_S|$ , resulting in a shorter settling time and therefore into sharper vertical lines on the screen. Higher values of  $|k_S|$  can even be adjusted by the capacitor  $C_{EXT}$ , however, the chosen  $\tau_s$  just minimizes the power dissipation in the external transistor.

Beside these differences, concerning the driving condition and settling behaviour, the now solution significantly improves the reliability of the complete deflection circuit. The built in collector and base current limitation together with an undervoltage sense, optimally protects the power element during the turn ON and OFF phase of the cassis. An improved breakdown characteristic of the power transistor during the flyback phase results from a more negative base polarization compared with the transformer solution. This negative voltage can easily be adjusted by the external base  $R_B$   $C_B$  network (Fig. 7). Additionally, the SYN DET input avoids any base turn ON current during the flyback otherwise the power transistor could be damaged.

Fig. 11 - Measured collector and base currents

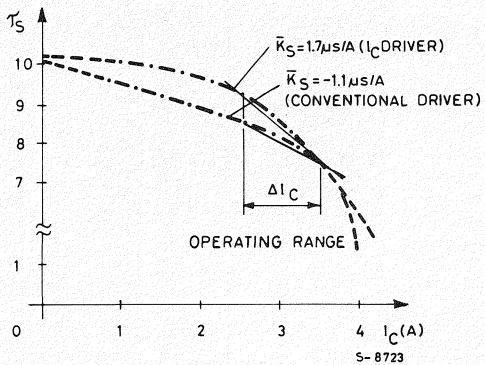


A conventional driver circuit must carefully be adapted to a given deflection circuit and only operates for a fixed deflection frequency. Contrarily, the integrated solution is widely independent of the deflection frequency and offers a high flexibility.

In order to adjust the turn on overdrive and the storage time, respectively the settling time, one must only define the sense resistor  $R_S$  (0.1-0.3 $\Omega$ ) and the capacitor  $C_{EXT}$  (0.5-2nF).

A more complete survey which summarizes the features of both concepts is presented in Tab 1. Although the transformer solution can realize an impedance matching, whereas the integrated element operates as a series pass regulator, the total power dissipation is even smaller in the new solution.

Fig. 12 - Illustration of the stability factor  $K_S$  TABLE 1 - Table of key performance summary



Characteristics	TDA 8140 TDA 8143	Conventional Driver
RELIABILITY		
$I_C$ limitation	yes	no
$I_B$ limitation	yes	yes
Undervoltage sense	yes	no
Flyback disable	yes	no
Neg. $V_{BE}$ (Turn OFF)	-2V to -6V	-2V
DEFLECTION FREQUENCY	independent	fixed design
APPLICATION ADAPTATION	one R, one C	several R, C transformer
SETTLING TIME	short (adjustable)	fixed
COMPONENTS	5 to 7	10 to 15
TOT. POWER DISS. (30AX, $f_C = 3.2A$ )	2.5W	3.2W